Design and Analysis of Rolled Rotor Switched Reluctance Motor

Eyhab El-Kharashi*

Abstract - In the conventional SRM with multi-rotor teeth, the air gap must be very small in order to drive the SRM in the saturation region that is necessary for high output torque. However, this leads to the problem of overheating; particularly in the case of a small-size SRM. This paper discusses the design of a new type of SRM, namely the rolled rotor SRM. This new type does not require more than a single region of a very small airgap. This solves the overheating problem in the small size SRM. Moreover, the use of the rolled rotor, instead of the conventional toothed rotor, grades the airgap region in a fashion that gives a smooth variation in the reluctance and smooth shapes of both current and torque. The latter functional behavior is required in many applications such as servo applications. The paper first addresses general design steps of the rolled rotor SRM then proceeds to the simulation results of the new SRM in order to evaluate the advantages gained from the new design. In addition, this paper compares the torque ripples obtained from the new design to its equivalent conventional one.

Keywords: Rolled rotor, Switched reluctance motor, Finite element, Smooth reluctance variation, Torque ripples minimization, Modeling, Matlab software

1. Introduction

The electric motors used in driving applications are the induction motors, the permanent magnet motors and the switched reluctance motors (SRM). The permanent magnet motors have the disadvantage of requiring of expensive magnets. The induction motors are prone to high copper losses in both the rotor and the stator. Therefore, the focus of motor designers shifts to the SRM due to its high specific output torque (torque/volume) and the absence of any type of copper windings or permanent magnets on the rotor or brushes [1].

Fig.1 shows the cross section of a 6/4 short-pitch conventional SRM and the Flux-Linkage trajectory under current control. The area between the aligned and the unaligned positions is proportional to the output torque. The SRM must work in deep saturation region in order to deliver significant output torque. Hence, the air gap must be very small. The requirement of a minimum possible airgap puts the SRM at disadvantage due to potential overheating. As a solution, the SRM is not usually loaded its full capacity, as a means to obviate overheating. This paper is intended to introduce a new design of the SRM that possesses only one small region of airgap, without compromising performance. The expected performance is at the same level of the conventional toothed-rotor.

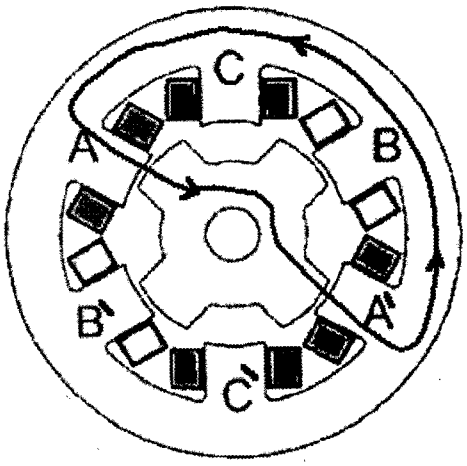

Fig. 1.a Cross Section of a 6/4 Short-Pitch SRM

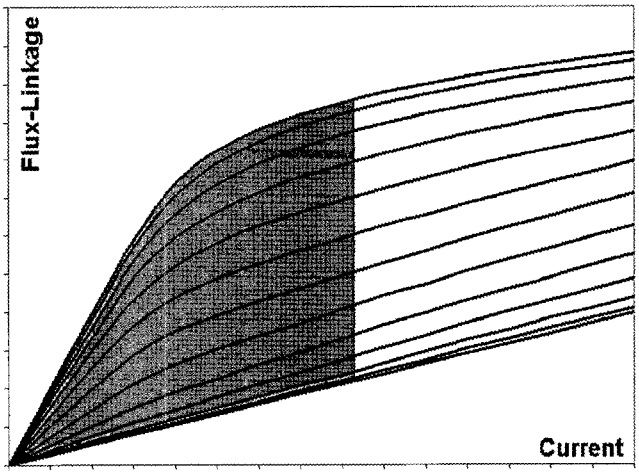

Fig. 1.b Flux-Linkage Characteristic under Current Control

* Dept. of Electrical Power Engineering, Ain Shams University, Cairo, Egypt (EyhabElkharahi@hotmail.com)
Received February 26, 2006 ; Accepted November 9, 2006

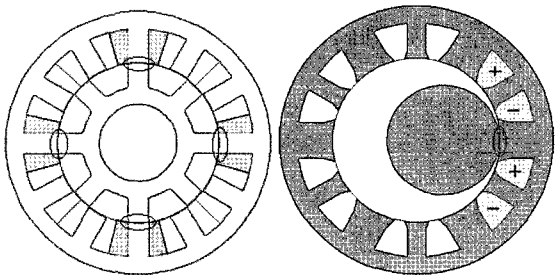

2.a **2.b**

Fig. 2 The Regions of the Narrow Airgaps in both Designs

Fig. 2.a shows the regions of narrow airgap in a 12/8 conventional toothed-rotor SRM. There are four regions of narrow airgap in the aligned position. To the contrary, the rolled rotor SRM (Fig. 2.b) has only one region of narrow airgap. In addition, the airgap in the rolled rotor SRM is graded in order to avoid overheating. The rolled rotor has a smooth variation in the reluctance and, consequently, a smooth shape of current and torque when the switch-on angle is selected properly [2]-[3]. The paper presents the simulation results of the new design and its comparison with its equivalent conventional SRM. A Matlab/Simulink program is used to simulate the functioning of the new SRM and to test its dynamic performance under different operating conditions.

2. Theoretical Background

If one phase of the stator of the rolled rotor SRM is switched on, the rolled rotor sees all the positions as unstable, except for the position of minimum reluctance - or maximum inductance. The rolled rotor moves directly from any position to this stable position. The minimum reluctance position is located in front of the energized phase such that the rolled rotor can align itself with this energized phase. The unaligned position is the position of minimum inductance, which is diametrically opposite to the energized main wide flux tooth. A half mechanical cycle is completed if the rotor rotates from the unaligned position to the aligned position.

There are two trends that influence the selection of the rotor's diameter. First, the diameter of the rotor is directly proportional to the output torque. But a rotor with a large diameter minimizes the gap between the maximum inductance and the minimum inductance and, consequently, decreases the output torque. In addition, large rotor diameter makes the rotor heavier; thus increasing the rotor iron losses, and putting some limitation on the maximum running speed of the rotor. Second, small rotor diameter reduces output torque but the rotor's light weight enables it rotate at high speeds with minimal iron losses. Based on these trends, there exists an optimum rotor diameter. Next section is dedicated to the formulation of an approximate method for determining the best diameter of the rolled rotor SRM.

Prior to discussing the design process of the rolled rotor SRM, it is noteworthy that the SRM is in general a highly non-linear electric motor. Therefore, an accurate prediction of the magnetic circuit parameter as well as the static torque characteristics of this motor requires the use of an adaptive two dimensions finite element [4].

A twelve teeth stator is hereafter considered. The six wide teeth carry the main flux of the machine and the rest are return flux paths. The width of the main flux tooth is double the return flux tooth width.

Fig.3 shows the stator of the proposed new SRM, the width of the main flux tooth is double that of the return flux path. This is intended to increase the flux crossing from the stator to the rotor cylinder in the aligned position.

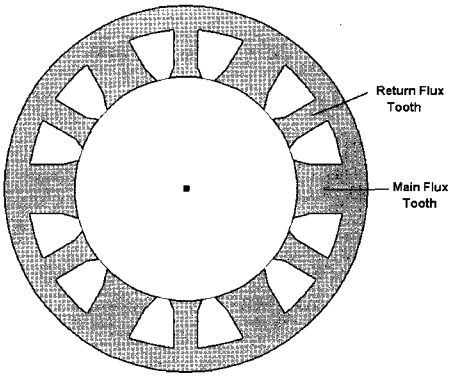

Fig. 3 The Stator of the Proposed New SRM

The rotor of this new SRM is a cylindrical iron rotor. It has an outside diameter less than the stator bore diameter. Its centre is shifted from the centre of the stator. That makes the air gap length vary (narrow in some regions and wide in other regions). Accordingly, the variation in the reluctance produces reluctance torque. Fig. 4 shows the windings distribution in the stator. The proposed rolled rotor SRM has three phases in the stator each phase fills four stator slots (two coils per phase).

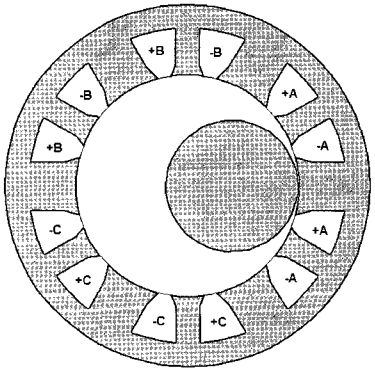

Fig. 4 Windings Distribution

3. Determination of the Optimum Rotor Diameter

Fig. 5 shows the unaligned position of the proposed new design of the SRM; the rotor is in the position of minimum inductance which is at the opposite side of the same diameter of the main energized wide tooth.

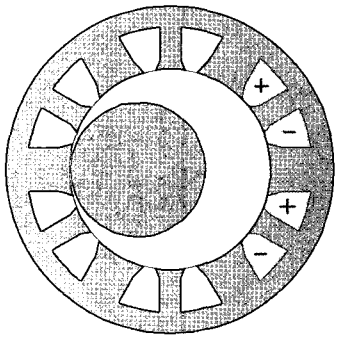

Fig. 5 Rotor Diameter = 0.68 Stator Bore Diameter (Unaligned Position)

When one stator phase is energised, the rotor sees all the positions as unstable except for one position - the maximum inductance (the aligned position). The rotor rotates from any position to stand in front of the energised wide tooth in order to reach a minimum reluctance position. Fig. 6 shows the windings of an energized one phase and the rotor aligning itself to this position.

The area between the aligned position and the unaligned position, in the Flux-Linkage/Current characteristic of the proposed new SRM, is proportional to the output torque. Thus, the area enclosed between these two lines gives an indication about the output torque of any design of this new SRM.

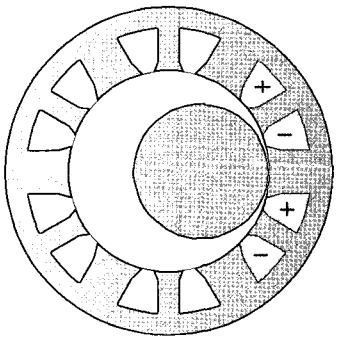

Fig. 6 Rotor Diameter = 0.68 Stator Bore Diameter (Aligned Position)

Fig. 4 shows the rotor diameter equals 0.6 the stator bore diameter. Fig. 5 and Fig.6 show the rotor diameter equals 0.68 the stator bore diameter. Fig. 7 shows the rotor diameter equals 0.95 the stator bore diameter.

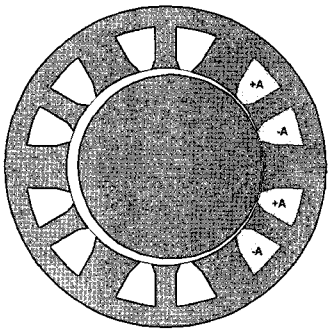

Fig. 7 Rotor Diameter = 0.95 Stator Bore Diameter (Aligned Position)

In the case shown in Fig. 4, the rotor is relatively small; hence, it produces low torque. In Fig. 7, the rotor is too big such that a small variation in the reluctance between the aligned and the unaligned position can reduce the output torque and can create considerable losses.

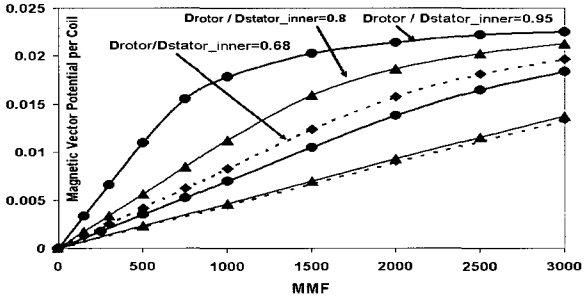

Fig. 8 Comparing the Characteristics of Different Rotor Diameters

Fig. 8 shows a comparison between the aligned and the unaligned positions for different designs of the rolled rotor SRM. All SRM's have the same stator dimensions, while the only change is in the rotor diameter.

The small rotor diameter delivers relatively low torque (the area enclosed between the aligned and the unaligned position is proportional to the output torque). Increasing the rotor diameter increases the area between the aligned and the unaligned position until the ratio between the rotor diameter to the stator bore diameter equal 0.8. Increasing the rotor diameter beyond this ratio would slightly increase the enclosed area. Hence, the best rotor diameter =0.8 stator bore diameter. Expectedly, any increase beyond this ratio would result in a negligible improvement in the output torque. However, it considerably increases the weight of the rotor in addition to the rotor iron losses [5].

4. Complete Details of the Proposed New Design

Based on the previous section, the rotor diameter is selected to be 0.8 the stator bore diameter.

4.1 Aligned Position

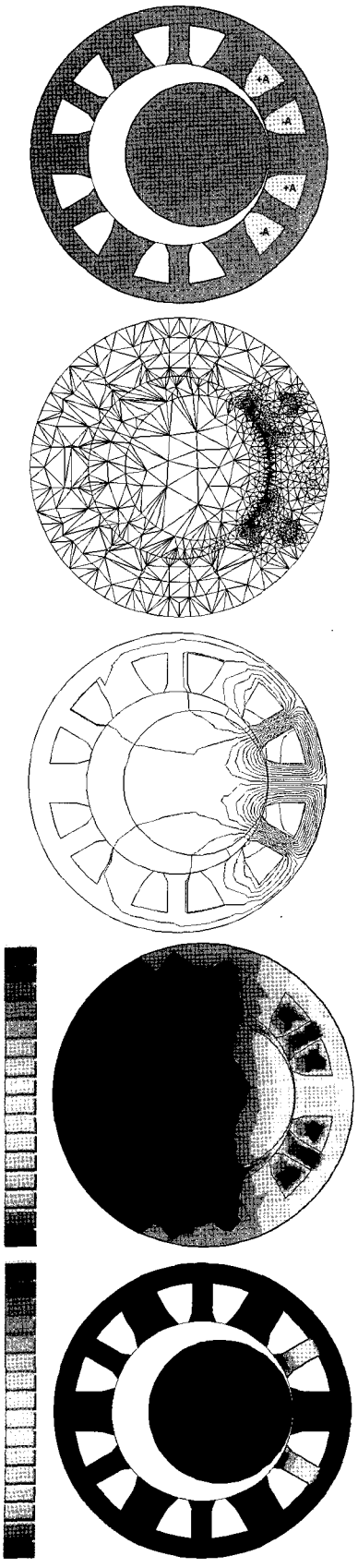

Fig. 9 Aligned Position of the New Design

Fig. 9 shows the aligned position of the new design of the rolled rotor SRM along with its adaptive mesh. The magnetic flux plot, the flux density and the saturation are all shown at 3000MMF per slot. In the aligned position the cylindrical rotor moves from any position to align itself at the energized phase [6].

4.2 Unaligned Position

Fig. 10 shows the unaligned position of the proposed new design along with its adaptive mesh. The magnetic flux plot, the flux density, and the saturation are all shown at 3000MMF per slot. The unaligned position occurs when the rotor is in a position of maximum reluctance with respect to the energized phase.

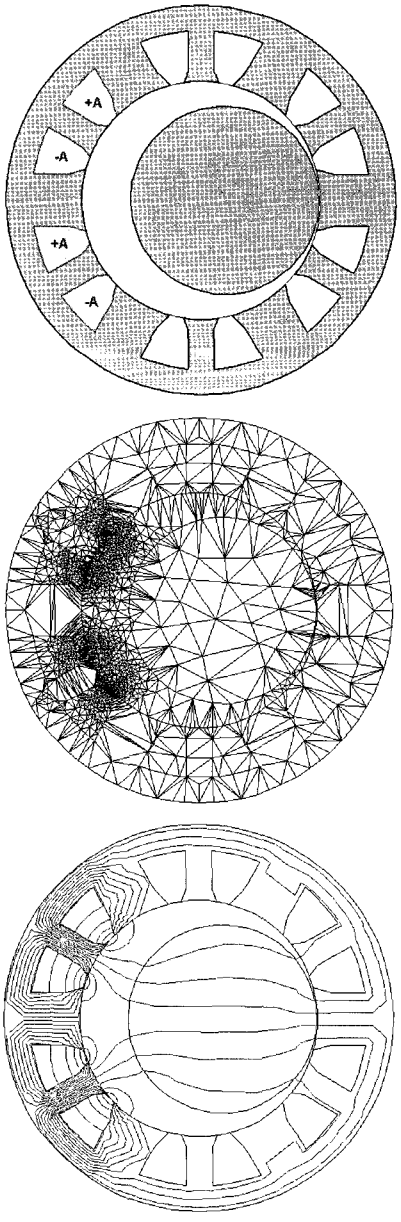

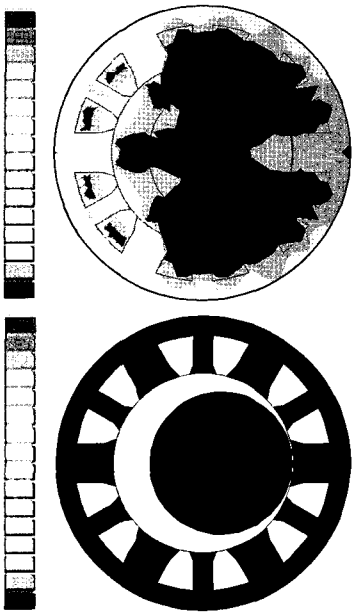

Fig. 10 Unaligned Position of the New Design

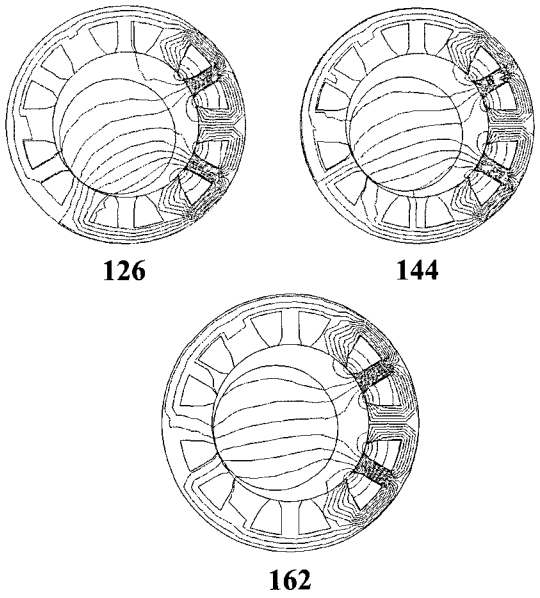

Fig. 11 New Rolled Rotor Models in a Range of Rotor Positions

5. Determining the Flux-Linkage Characteristic

As shown in Fig. 11 different models are built using 2D adaptive finite element for different rotor positions in order to accurately determine the characteristics of the magnetic vector potential (figure12, [6]).

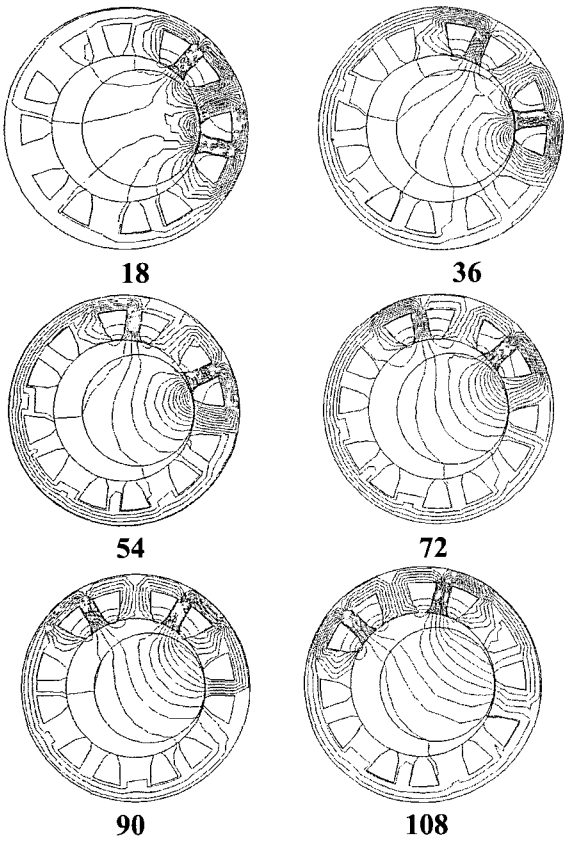

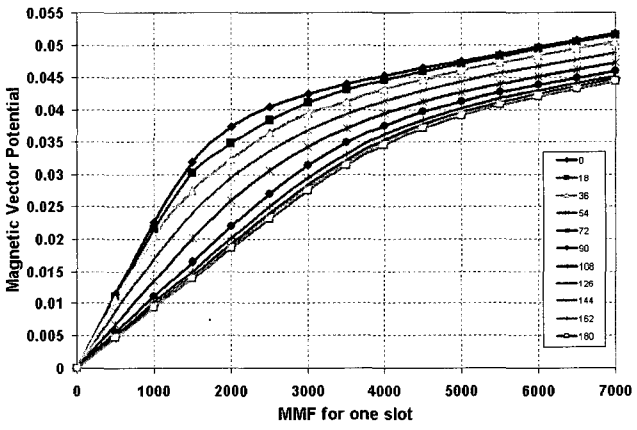

Fig. 12 Magnetic Vector Potential for the Rolled Rotor SRM for different Rotor Positions

6. The Flux-Linkage Characteristic and the Static Torque Characteristic

The flux linkage characteristic can be obtained from the magnetic vector potential characteristic, assuming a specific number of turns. There are six coils, two for each phase. Assume the number of turns of each coil to be 300, 150 conductors per slot. Fig. 13 shows the Flux-Linkage characteristic of the proposed new design for 150 conductors per slot [7],[8],[9]. Fig. 14 presents the static torque characteristic for the new rolled rotor SRM. As shown, the torque increases and decreases smoothly. The static torque characteristic can be obtained from the following equation [10]:

$$T(\theta,i)=\left.\frac{dW'(\theta,i)}{d\theta}\right|_{i=const} \quad (1)$$

(Assuming 150 conductors per slot)

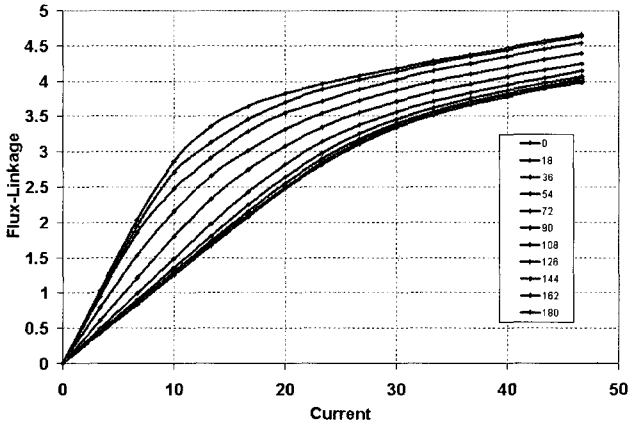

Fig. 13 Flux-Linkage Characteristic of the New Rolled Rotor SRM

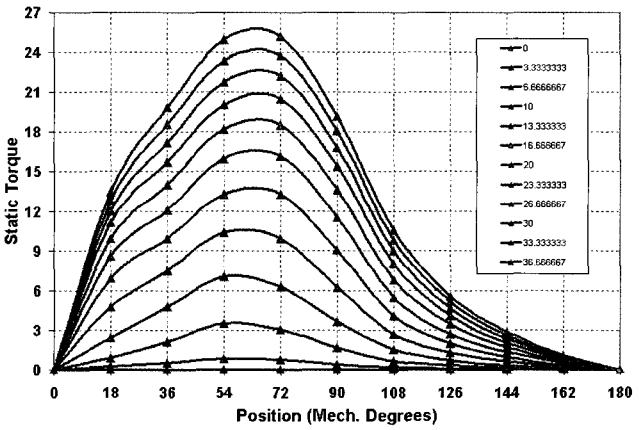

Fig. 14 Static Torque Characteristic of the New Rolled Rotor SRM

7. Minimization of the Torque Ripple in the New Design

In this section the torque ripple in the new rolled rotor SRM is compared to the conventional 12/8 SRM in order to determine the percentage reduction in the torque ripples due to the use of this rolled rotor which smoothed the air gap.

Fig. 15 shows the static torque characteristic of the conventional 12/8 toothed-rotor SRM and the torque ripples between two phases. In general, the torque ripples in the SRMs is defined as the percentage difference between two values of the torque in the static torque characteristic. The first value is the maximum value of the torque and the second is the torque at the point of intersection between the static torques of two different phases of the SRM. As shown in Fig. 15 the conventional SRM has eight poles in the rotor; hence the mechanical cycle is 45 mechanical degrees. The conventional SRM has three phases of windings on the stator, such that each phase is shifted 15 mechanical degrees from the other.

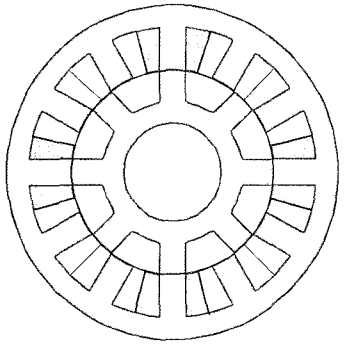

a) Cross Section of 12/8 Conventional SRM, the Location of One Phase Windings is shown

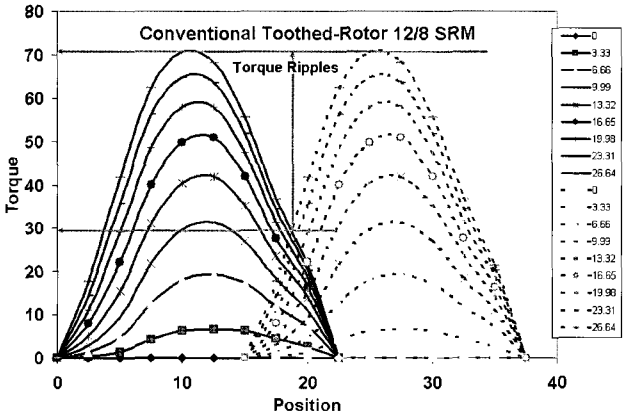

b) The Static Torque Characteristic for Two Phases

Fig. 15 Static Torque Characteristic of 12/8 Conventional SRM and the Torque Ripple between Two Phases

Indicated in Fig. 15 are the static torque characteristic for two different phases and the point of intersection. By substituting in the torque ripples formula (Equation 2,[11]), the percentage ripple is found to be 59.15%:

$$\text{Percentage Ripples} = \frac{T_{maximum} - T_{intersection}}{T_{maximum}} \quad (2)$$

Fig. 16 shows the static torque characteristic of the new SRM and the torque ripples between two phases. Similarly, the torque ripple of the new SRM can be calculated according to Equation 2. The percentage ripple is 26.92%. It is evident from the previous calculations that the use of the rolled rotor significantly reduces the percentage ripples in the torque characteristic.

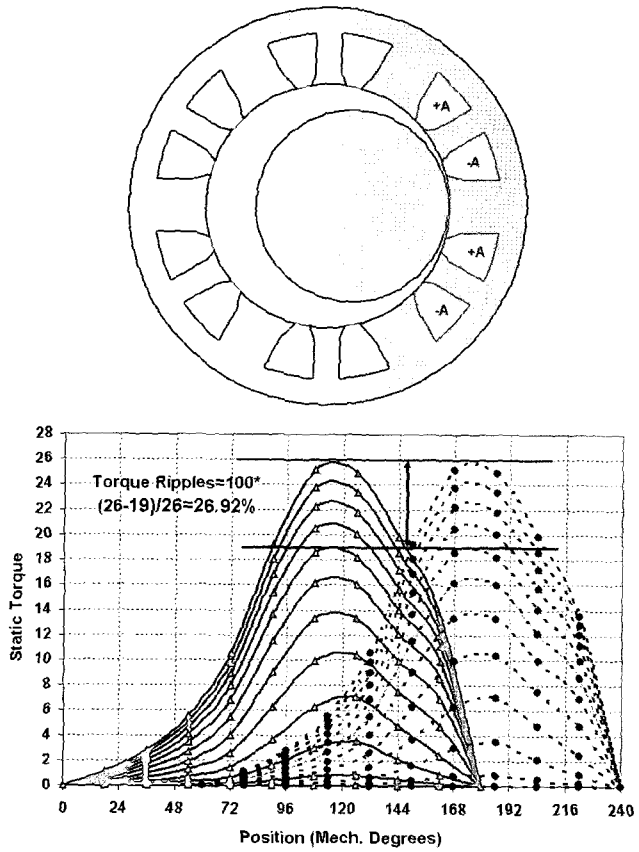

Fig. 16 Static Torque Characteristic of New Rolled Rotor SRM and the Torque Ripple between Two Phases

8. The Simulation of the New Rolled Rotor SRM

The machine performance can be analytically predicted by means of the fundamental equation of the terminal voltage of any SRM [12]:

$$v = R \cdot i + \frac{\partial \psi}{\partial t} \tag{3}$$

Then by solving one of the following 1st order differential equations:

$$\begin{aligned} v &= R \cdot i + \frac{di}{dt} \cdot \frac{\partial \psi}{\partial i}(\theta,i) + \omega \cdot \frac{\partial \psi}{\partial \theta}(\theta,i) \\ v &= R \cdot i + \frac{di}{dt} \cdot \frac{\partial \psi(\theta,i)}{\partial i} + \omega \cdot \frac{\partial \psi(\theta,i)}{\partial \theta} \\ v &= R \cdot i + \frac{di}{dt} \cdot L(\theta,i) + \omega \cdot i \cdot \frac{\partial L}{\partial \theta}(\theta,i) \\ v &= R \cdot i + \frac{di}{dt} \cdot L(\theta,i) + \omega \cdot i \cdot \frac{dL(\theta,i)}{d\theta} \end{aligned} \tag{4}$$

A numerical approach to the simulation of SRMs has been introduced in [12]-[13]. The flux-linkage can be calculated as follows:

$$\psi = \int (v - R \cdot i(\theta,\psi))\delta t \tag{5}$$

The torque can be obtained indirectly from the co-energy, as follows:

$$W'(\theta,i) = \int_0^i \psi(\theta,i)di \Big|_{\theta=const} \tag{6}$$

$$T(\theta,i) = \frac{dW'(\theta,i)}{d\theta}\Big|_{i=const} \tag{7}$$

Fig. 17 is the block diagram of the SRM simulation package. The flux linkage characteristic data are taken from the adaptive finite element solution of the magnetic characteristics; then they are stored in tables (one for the flux-linkage characteristic and the other for the torque); the tables are loaded into the simulation of the SRM using Matlab/Simulink [14].

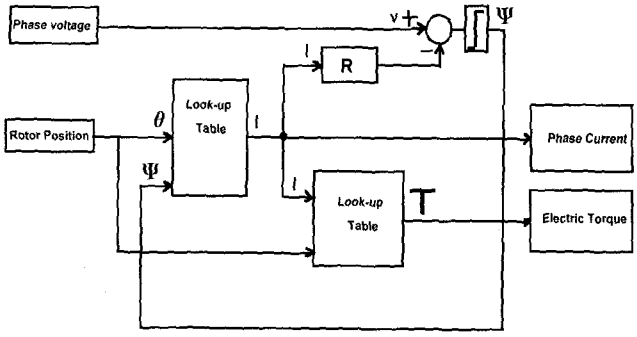

Fig. 17 Block Diagram of SRM Simulation

9. Dynamic Performance at low Speed

Matlab/Simulink is used to generate the simulated dynamic response of the new SRM at low speeds of rotation (500 rpm). The DC voltage of the converter is 600 volts and the switching On/Off angles are -60/60 degrees (mechanical angles). Fig. 18 shows torque versus position at low speed, while the advance switching is at angle 60 degrees. Fig. 19 shows torque versus position at low speed and, while the advance switching is at angle 10 degrees. It is noted that the average torque in the latter case is higher than the former case [15].

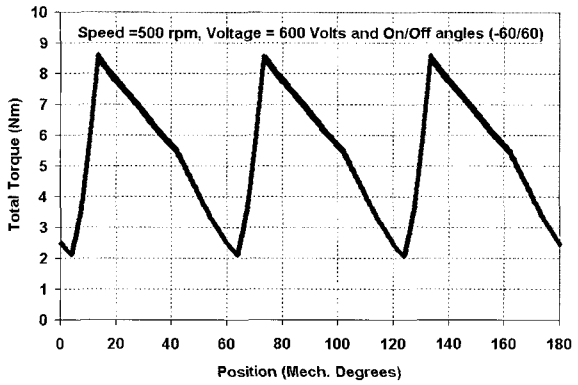

Fig. 18 Torque versus Position Switching On Angle before the Unaligned Position by 60 Degrees (Low Speed)

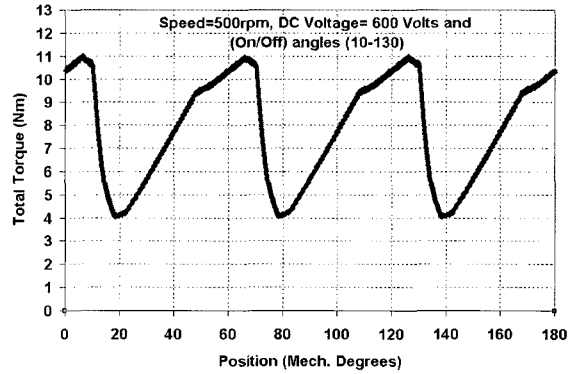

Fig. 19 Torque versus Position Switching On Angle after the Unaligned by 10 Degrees (Low Speed)

10. Dynamic Performance at high Speed

Matlab/Simulink is used here to obtain the simulated dynamic response of the new SRM at high speed (1500 rpm). The DC voltage of the converter is 600 volts and the switching On/Off angles are 10/130 degrees (mechanical angles). Fig. 20 shows simulated results of the new SRM at high speed (1500 rpm), DC voltage 600 volts with a Switching-On angle that follows after the unaligned position by 10 degrees.

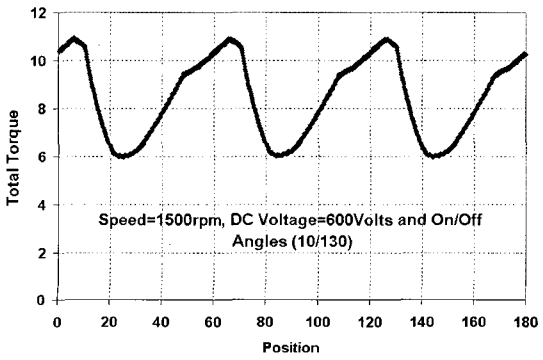

Fig. 20 a) Torque versus Position

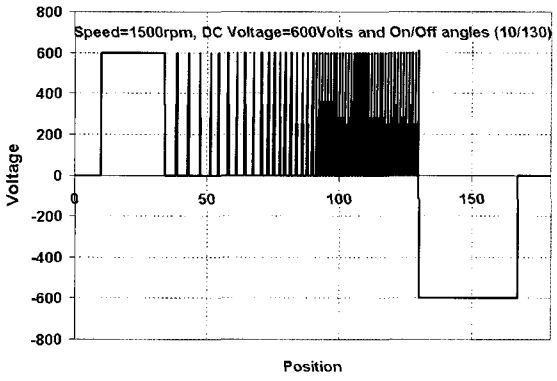

Fig. 20 b) Voltage versus Position

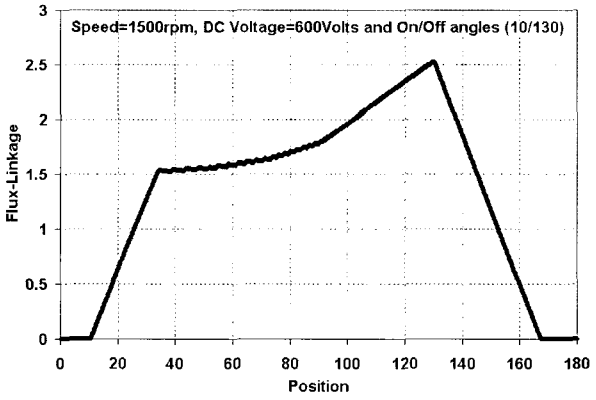

Fig. 20 c) Flux-Linkage versus Position

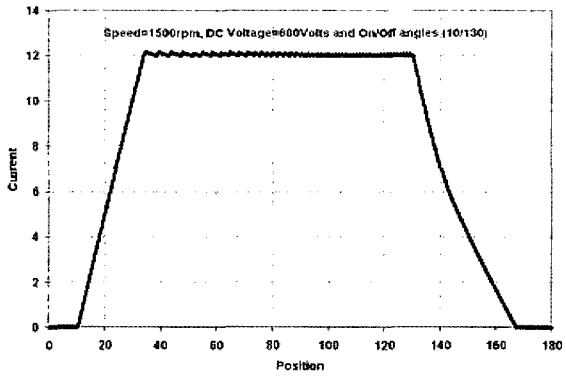

Fig. 20 d) Curent versus Position

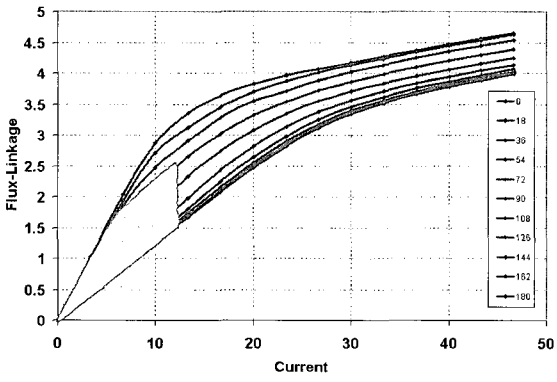

Fig. 20 e) Flux-Linkage Trajectory

Fig. 20 Simulated Dynamic Performance of the New SRM at high Speed Operation

11. Torque Speed Envelope

Fig. 21 shows the torque speed envelope for the new SRM. The new SRM has an excellent torque/speed envelope, whereby the machine can deliver strong output torque at relatively high speed.

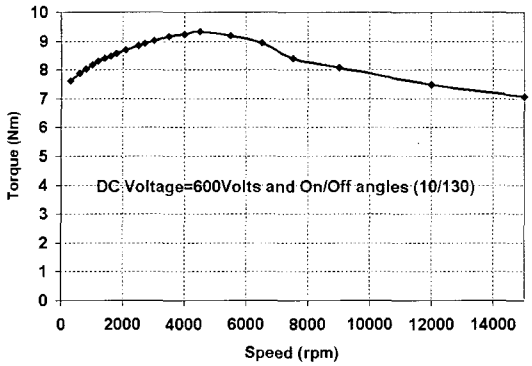

Fig. 21 Torque speed Envelope for the Rolled Rotor SRM

12. Changing the Connection of the two Coils of Each Phase

Fig. 22 shows a scheme of the change in polarity of the second coil of the energized phase. Fig. 23 shows the aligned and the unaligned position at the two different connections of the second coil of the energized phase. The aligned position comes up after changing the connection. This results in a small increase in the output torque [16].

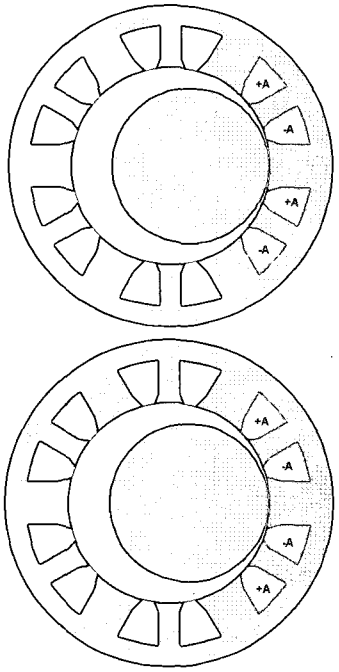

Fig. 22 Changing the Connection of the two Coils of Each Phase

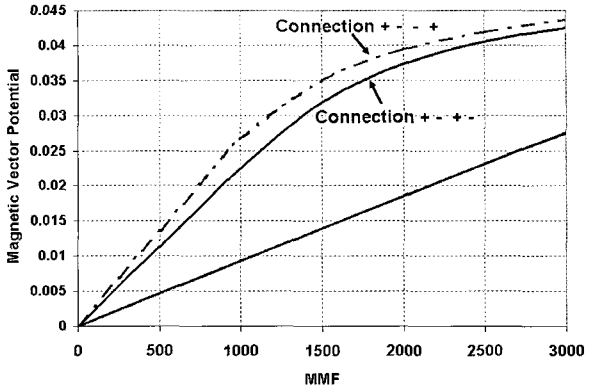

Fig. 23 The Aligned and the Unaligned Positions for the different connections

13. Tables

Table 1 Dimensions of the New Rolled Rotor SRM

Stator Axial Length	150 mm
Stator Outside Diameter	150 mm
Stator Core Back	10 mm
Height of Stator Poles	21.12 mm
Width of Stator Pole : Maximum	20 mm
Width of Stator Pole : Minimum	10 mm
Rotor Diameter	36.32 mm
Air Gap Width : Minimum	0.3 mm
Air Gap Width : Maximum	18.47 mm

Table 2 Dimensions of the Conventional 12/8 SRM

Stator Axial Length	150 mm
Stator Outside Diameter	150 mm
Shaft Diameter	43.64 mm
Rotor Diameter	90.8 mm
Air Gap Width	0.3 mm
Stator Core Back	10 mm
Rotor Core Back	10 mm
Stator Tooth Width	11.76 mm
Rotor Tooth Width	11.76 mm

14. Conclusions

This paper introduces a new design of the switched reluctance motor. The conventional toothed rotor is replaced by a solid iron cylinder. The main objective of this replacement is to change the topology of the magnetic circuit in a way that enhances the performance of the new design over the conventional SRM. The new rotor reduces the potential overheating in addition to the total material losses. Accordingly, the SRM can accommodate more loading due to the increase in thermal limits. In addition, this configuration of the rotor smoothes the air gap, resulting in smooth shapes of the current and the torque.

The latter is traditionally required in some practical cases such as servo applications. The paper used the adaptive finite element in the prediction of the characteristics of the rolled rotor SRM. The flux linkage characteristic was predicted and the torque characteristic was calculated from it.

Then the paper examined the new design of the SRM by analyzing the percentage reduction in the torque ripples due to the use of the new SRM. The paper used the Matlab/Simulink module to simulate the dynamic performances for different modes of SRM operation (low speed and high speed). The generated torque/speed envelope shows excellent characteristics as to the capability of the new SRM to maintain its torque at very high speeds - as opposed to the conventional SRM. It can be concluded that the new design can replace the conventional design of the SRM in attempt to resolve some problems of overheating along with improved functionalities.

References

[1] J. R. Gyorki. Design Secrets of Switched Reluctance Motors. September 26, *J. Machine Design*, 1996.

[2] E. A. Fisher, E. Richter. Conical Rotor for Switched Reluctance Motor. *US5233254, US-Patent*, 3/8/1993.

[3] T. J. E. Miller. Optimal Design of Switched Reluctance Motors. *IEEE Transactions on Industrial Electronics*, February 2002: 49(1).

[4] K. M. Richardson, C. Pollock and J. O. Flower. Design of a Switched Reluctance Sector Motor for an Integrated Motor/Propeller Unit. *IEE Electrical Machines and Drives*' 11-13 September 1995.

[5] A. Michaelides and C. Pollock. Design and performance of a high efficiency 5-phase switched reluctance motor. *IEEE conference of Electrical Machines and Drives,* 11-13 September 1995.

[6] A. R. Eastham, H. Yuan, G. E. Dawson, P. C. Choudhuhury, P.M. and Cusack. A Finite Element Evaluation of Pole Shaping in Switched Reluctance Motors. *Electrosoft*, 1990: 1(1).

[7] A. Matveev, T. Undeland, R. Nilssen. Design Optimisation Of Switched Reluctance Drives Using Artificial Neural Networks. *EPE-PEMC 2002* Dubrovnik & Cavtat.

[8] J. Reinert, R. Inderka, M. Menne, and R. W. De Doncker, 'Optimisation Performance in Switched Reluctance Motor' *IEEE Industry Applications Magazine*, July/August 2000.

[9] M. Sanada, S. Morimoto, Y. Takeda and N. Matsui, 'Novel Rotor Pole Design of Switched Reluctance Motors to Reduce the Acoustic Noise' *IEEE Conf. IA 2000*, Italy.

[10] M. R. Harris, A. Hughes, and P. J. Lawrenson, 'Static Torque Production in Saturated Doubly-Salient Machines', *Proc. IEE*, 1975, 122, (10), pp. 1121-1127.

[11] R. S. Wallace and D. G. Taylor, 'Three Phase Switched Reluctance Motor Design to Reduce Torque Ripple' *International Conference on Electrical Machines* ICEM'90, Pages: 782-787.

[12] U. Bock, 'A Novel Approach of Modeling SR Motor Systems' ICEM 2002, *15th International Conference on Electrical Machines*' Brugge, Belgium, August 25-28, 2002.

[13] L. Xu and E. Ruckstadter, 'Direct Modelling of Switched Reluctance Machine by Coupled Field-Circuit Method' *IEEE Transactions on Energy Conversion*, Vol. 10, No. 3, September 1995.

[14] A. Michaelides and C. Pollock, 'Modelling of a New Winding Arrangement to Improve Performance in the Switched Reluctance Motor', *IEE Conference of Electric Machines and Drive*, 1993.

[15] Fulton, N. Neilson, 'Operation of Switched Reluctance Machines' European Patent, *EP 0959555, 24/11/1999.*

[16] D. A. Staton, W. L. Soong and T. J. E. Miller, 'Unified Theory of Torque Production in Switched Reluctance and Synchronous Reluctance Motors' *IEEE Transactions on Industry Applications*, Vol. 31, No. 2, March/April 1995.

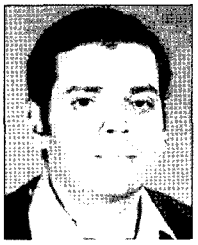

Eyhab El-Kharashi

He Received his PhD degree in the electrical machines design from University of Newcastle upon Tyne, UK in 2003 and B.Sc. (first class honours) and M.Sc. degrees in electrical Power and Machines Engineering from Ain Shams University, Cairo, Egypt, in 1994 and 1997 respectively. Now he is an assistant professor in the Department of Electrical Power and Machines, Faculty of Engineering, Ain Shams University, Cairo, Egypt. His research interests include electrical machines design.